Atmospheric
Chemistry
and Physics

Open Access

Simultaneous reductions in emissions of black carbon and co-emitted species will weaken the aerosol net cooling effect

Z. L. Wang[1,2]**, H. Zhang**[2,3]**, and X. Y. Zhang**[1,4]

[1]Chinese Academy of Meteorological Sciences, Beijing, China
[2]Collaborative Innovation Center on Forecast and Evaluation of Meteorological Disasters,
Nanjing University of Information Science and Technology, Nanjing, China
[3]Laboratory for Climate Studies, National Climate Center, China Meteorological Administration, Beijing, China
[4]Key Laboratory for Atmospheric Chemistry, Chinese Academy of Meteorological Sciences, Beijing, China

Correspondence to: X. Y. Zhang (xiaoye@cams.cma.gov.cn)

Abstract. Black carbon (BC), a distinct type of carbonaceous material formed from the incomplete combustion of fossil and biomass based fuels under certain conditions, can interact with solar radiation and clouds through its strong light-absorption ability, thereby warming the Earth's climate system. Some studies have even suggested that global warming could be slowed down in the short term by eliminating BC emission due to its short lifetime. In this study, we estimate the influence of removing some sources of BC and other co-emitted species on the aerosol radiative effect by using an aerosol–climate atmosphere-only model BCC_AGCM2.0.1_CUACE/Aero with prescribed sea surface temperature and sea ice cover, in combination with the aerosol emissions from the Representative Concentration Pathways (RCPs) scenarios. We find that the global annual mean aerosol net cooling effect at the top of the atmosphere (TOA) will be enhanced by $0.12\,\mathrm{W\,m^{-2}}$ compared with recent past year 2000 levels if the emissions of only BC are reduced to the level projected for 2100 based on the RCP2.6 scenario. This will be beneficial for the mitigation of global warming. However, both aerosol negative direct and indirect radiative effects are weakened when BC and its co-emitted species (sulfur dioxide and organic carbon) are simultaneously reduced. Relative to year 2000 levels, the global annual mean aerosol net cooling effect at the TOA will be weakened by 1.7–$2.0\,\mathrm{W\,m^{-2}}$ if the emissions of all these aerosols are decreased to the levels projected for 2100 in different ways based on the RCP2.6, RCP4.5, and RCP8.5 scenarios. Because there are no effective ways to remove the BC exclusively without influencing the other co-emitted components, our results therefore indicate that a reduction in BC emission can lead to an unexpected warming on the Earth's climate system in the future.

1 Introduction

Aerosols in the atmosphere can alter the amount of sunlight reaching the Earth, perturb the temperature structure of the atmosphere, and influence cloud cover by directly scattering sunlight (e.g., sulphate, organic carbon (OC) and nitrate) or absorbing it (e.g., black carbon (BC) and dust) (Boucher et al., 2013). Aerosol particles can also change cloud microphysical and optical properties by acting as cloud condensation nuclei (CCN) or ice nuclei (Twomey, 1977; Albrecht, 1989; DeMott et al., 1997). These changes due to aerosols will directly or indirectly affect the climate. Since the start of the industrial era, an increase in atmospheric aerosol emissions has likely led to a net cooling of the Earth's climate system (Boucher et al., 2013).

BC has a special role in the climate system, although it accounts for less than 5 % of the mass of atmospheric aerosol in most areas of the world (X. Y. Zhang et al., 2012). BC can increase the amount of solar radiation absorbed within the Earth's climate system and heat the atmosphere or surface by directly absorbing sunlight in the visible to infrared wavebands (Hansen et al., 2000; Ramanathan and Carmichael, 2008), changing the cloud amount and its brightness due to

embedding into clouds (Chuang et al., 2002; Koch and Del Genio, 2010; Jacobson, 2012; Wang et al., 2013a), or by reducing the surface albedo due to deposition onto snow and ice surfaces (Wang et al., 2011; Lee et al., 2013). BC has even been considered as a potential cause of global warming (Hansen et al., 2000; Jacobson, 2010; Bond et al., 2013). Ramanathan and Carmichael (2008) compared the radiative forcings of greenhouse gases and BC, suggesting that the direct radiative forcing due to BC was larger than that due to any other greenhouse gas except CO_2. The radiative heating effect on the whole atmosphere due to BC was almost double that due to all greenhouse gases. By considering all the known ways that BC affects the climate system, Bond et al. (2013) gave an estimate of industrial-era climate forcing of $+1.1 \, \mathrm{W \, m^{-2}}$ due to BC with 90 % uncertainty limits of $+0.17$ to $+2.1 \, \mathrm{W \, m^{-2}}$. BC can therefore be considered the second most important anthropogenic positive radiative forcing agent after CO_2 in the present-day atmosphere. Some studies have even suggested that global warming could be slowed down in the short term by eliminating BC emission due to its short atmospheric lifetime. For example, eliminating soot generated from fossil fuels, including BC, primary organic matter, and sulphate, was found to decrease global surface air temperature by 0.3–0.5° in the short term (about 15 year) (Jacobson, 2010). A simultaneous decrease of short-lived BC and methane through the adoption of control measures could reduce projected global mean warming by about 0.5° by 2050 (Shindell et al., 2012). However, there is a huge uncertainty and an ongoing debate in climate forcing of BC. Other studies, such as that by Myhre et al. (2013a), have much lower estimates of the direct radiative forcing from BC, which is reflected in the best estimate in the latest IPCC report (Boucher et al., 2013; Myhre et al., 2013b). Recent literature also suggests that the climate effect of BC may be overestimated due to overestimation of its lifetime (e.g., Hodnebrog et al., 2014; Samset et al., 2014; Q. Wang et al., 2014).

Reducing the emissions of absorptive aerosols (e.g., BC) would decrease the absorption of solar radiation by atmospheric aerosols, thereby enhancing the aerosol net cooling effect. However, BC, OC, sulphate, and some other aerosols have many common emission sources (e.g., in the emission sectors of transportation, industrial, residential, and commercial energy consumption, etc.), and they are generally co-emitted into the atmosphere (Lamarque et al., 2010). A technology-based global emission inventory of BC and OC showed that BC and primary OC particles were co-emitted from combustion including fossil fuels, biofuels, open biomass burning, and urban waste burning (Bond et al., 2004). An inventory of air pollutant emissions in Asia supporting the Intercontinental Chemical Transport Experiment-Phase B showed that sulfur dioxide (SO_2), BC, and OC all were emitted from power, industry, residential, and transportation sources (Zhang et al., 2009). A spatially resolved biomass burning data set also indicated that BC, OC, and SO_2 were proportionally emitted from biofuel and forest fire sources (Reddy and Venkataraman, 2002). Analyses of aerosol emission trends from some important source regions showed that there were same trends for BC, OC, and SO_2 separately emitted from fossil fuel, biofuel, and biomass burning sources from 1980 to 2009 (Chin et al., 2014), which indirectly suggested the co-emissions of BC with some other aerosols. Moreover, actual operational reduction in BC emission in most of severe polluted countries, like China, is often to cut the usage of coal and other fossil fuels, as well as forbid open burning to reduce biomass burning emissions. All these major measures will result in the emission reductions in BC and its co-emitted components at the same time.

Sulphate, BC, and OC are the main aerosol species in the atmosphere, and the emissions of sulphate and OC will be reduced accordingly if the emission of BC is reduced. Both sulphate and OC are strongly scattering and hygroscopic aerosols, and they can cool the climate system by directly scattering solar radiation and increasing the cloud albedo and lifetime by acting as CCN (Boucher et al., 2013). Therefore, would global warming necessarily be slowed down by reducing BC emission in the future? This is the point of this study.

Focusing on the issue mentioned above, the impact of removing some BC sources and other co-emitted species on the aerosol radiative effects was studied in this paper by using an aerosol–climate atmosphere-only model BCC_AGCM2.0.1_CUACE/Aero (Atmospheric General Circulation Model of Beijing Climate Center, BCC_AGCM2.0.1, coupled with the aerosol model of China Meteorological Administration Unified Atmospheric Chemistry Environment for Aerosols, CUACE/Aero) (Z. L. Wang et al., 2014) with prescribed sea surface temperature (SST) and sea ice cover (SIC), in combination with the Representative Concentration Pathways (RCPs) emission scenarios (van Vuuren et al., 2011) underpinning the Fifth Assessment Report of the Intergovernmental Panel on Climate Change (IPCC AR5). In Sect. 2, we introduce the aerosol–climate model and simulation details. In Sect. 3, we present the effects of reducing only BC emission and then of the simultaneous reduction of BC and other co-emitted aerosol emissions on aerosol direct, semi-direct and indirect, and net radiative effects. Finally, our discussion and conclusions are presented in Sect. 4.

2   Model and simulation

2.1   Model description

We use the aerosol–climate atmosphere-only model BCC_AGCM2.0.1_CUACE/Aero developed by Zhang et al. (2012a), and improved by Jing and Zhang (2013), Zhang et al. (2014), and Z. L. Wang et al. (2014) in this study. The aerosol direct, semi-direct, and indirect effects (albedo and lifetime indirect effects on stratiform clouds) have been included in BCC_AGCM2.0.1_CUACE/Aero. The model

has been used to study the impact of aerosol direct radiative effect on East Asian climate (Zhang et al., 2012a), direct radiative forcing of anthropogenic aerosols (Bond et al., 2013; Myhre et al., 2013a), climate response to the presence of BC in cloud droplets (Wang et al., 2013a), effect of non-spherical dust aerosol on its direct radiative forcing (Wang et al., 2013b), anthropogenic aerosol indirect effect (Z. L. Wang et al., 2014), and direct effect of dust aerosol on arid and semi-arid regions (Zhao et al., 2014).

A detailed description of BCC_AGCM2.0.1 was given by Wu et al. (2010). The model employs a horizontal resolution of T42 (approximately $2.8° \times 2.8°$) and a 26 layer hybrid sigma-pressure coordinate system in the vertical direction, with a rigid lid at 2.9 hPa. The time step is 20 min. However, the cloud overlap, radiation, and cloud microphysical schemes were improved in the model. The cloud overlap scheme of the Monte Carlo independent column approximation (McICA) (Pincus et al., 2003) and the Beijing Climate Center radiation transfer model (BCC_RAD) developed by Zhang et al. (2003, 2006a, b) were used instead of the old schemes in the model (Jing and Zhang et al., 2013). These schemes have improved the accuracy of the subgrid cloud structure and its radiative transfer process (Zhang et al., 2014). A two-moment bulk cloud microphysical scheme to predict both the mass and number concentrations of cloud droplets and ice crystals (Morrison and Gettelman, 2008) was implemented into the model instead of the old one-moment bulk cloud microphysical scheme (Z. L. Wang et al., 2014). The scheme of Abdul-Razzak and Ghan (2000) has been adopted for the activation of cloud droplets.

The aerosol model CUACE/Aero is a comprehensive module incorporating emission, gaseous chemistry, transport, removal, and size-segregated multi-component aerosol algorithms based on the Canadian Aerosol Module developed by Gong et al. (2002, 2003). A detailed description of CUACE/Aero was given by Zhou et al. (2012). The mass concentrations of the main five aerosols in troposphere, i.e., sulphate, BC, OC, dust, and sea salt, can be calculated. Each aerosol type is divided into 12 bins as a geometric series for a radius between 0.005 and 20.48 µm. Aerosol optical properties from Wei and Zhang (2011) and Zhang et al. (2012b) were calculated based on the Mie theory. The refractive indices of aerosols were adopted from d'Almeida (1991). Hygroscopic growth was considered for sulphate, OC, and sea salt (Zhang et al., 2012a).

2.2 Simulation details

Six simulations were run in this study. In all simulations, the model settings were the same, whereas aerosol emissions were different. All simulations kept greenhouse gas concentrations fixed at year 2000 levels in order to obtain the effect of change in aerosol emissions exclusively. Table 1 gives the emission setups in all simulations. As a base case, the first simulation (SIM1) used emissions of SO_2, BC, and OC for the year 2000, representing the aerosol effect for recent past. In the second simulation (SIM2), BC emission in 2100 under the RCP2.6 scenario was used, but the emissions of SO_2 and OC were the same as those in SIM1. In the third simulation (SIM3), BC emission in 2100 under the RCP2.6 scenario was also used, but the emissions of SO_2 and OC used were those for 2100 under the RCP8.5 scenario. In the fourth simulation (SIM4), the emissions of SO_2, BC, and OC for 2100 under the RCP2.6 scenario were used. In the fifth simulation (SIM5), BC emission in 2100 under the RCP2.6 scenario was used, but the emissions of SO_2 and OC used corresponded to the 2100 emission of BC under the RCP2.6 scenario by multiplying them with the ratios of the emissions of SO_2 and OC with BC in 2000. The ratios were calculated and applied for each individual grid box and month. In the sixth simulation (SIM6), the emissions of SO_2, BC, and OC in 2100 under the RCP4.5 scenario were used. Aerosol emission inventories from fossil fuel, biofuel, and biomass burning for the year 2000 given by Lamarque et al. (2010) were used. The emission data sets of RCPs scenarios were described by van Vuuren et al. (2011) and can be obtained from http://tntcat.iiasa.ac.at:8787/RcpDb/dsd?Action=htmlpage&page=about. The biomass burning emissions are also changed when using RCPs scenarios. The National Centers for Environmental Prediction (NCEP) reanalysis climatological data on a Gaussian grid were used as the initial field (downloaded from http://www.cesm.ucar.edu/models/atm-cam/download/). Data for the prescribed annual cycle of monthly mean SST and SIC based on the 21-year (1981–2001) climatology from the Hadley Centre (Hurrell et al., 2008) were used in these simulations. Each simulation was run for 20 years, and the simulation data for the last 10 years were averaged and analyzed.

The difference between SIM2 and SIM1 shows the impact on aerosol radiative effects (AREs) of reducing only BC emission maximally in the four RCPs scenarios. The difference between SIM3 and SIM1 indicates the effect of maximally reducing the emission of absorbing BC, combined with the least reduction in the emissions of precursor (SO_2) of scattering sulphate and OC on AREs. The differences between SIM4 and SIM1, between SIM5 and SIM1, and between SIM6 and SIM1 show the effects of a simultaneous reduction of SO_2, BC, and OC emissions under the RCP2.6 scenario, a reduction of the BC emission with a simultaneous reduction of the emissions of SO_2 and OC (in terms of their ratios with BC), and a simultaneous reduction in the emissions of SO_2, BC, and OC under the RCP4.5 scenario (representing a medium-low emission pathway), on AREs, respectively.

The aerosol direct effect (ADE) was obtained by calling the radiation routine two times (Ghan et al., 2012):

$$\Delta ADE = \Delta(F - F_{clean}), \tag{1}$$

where F is the radiative flux at the top of the atmosphere (TOA) and F_{clean} is the flux calculated as a diagnostic with

Table 1. Simulation setups.

Simulation	BC emission	OC and SO$_2$ emissions	Interpretation (compared to SIM1)
SIM1	year 2000	year 2000	recent past reference emissions
SIM2	RCP2.6 year 2100	year 2000	maximal reduction in BC; no reductions in OC and SO$_2$
SIM3	RCP2.6 year 2100	RCP8.5 year 2100	maximal reduction in BC; minimal reductions in OC and SO$_2$
SIM4	RCP2.6 year 2100	RCP2.6 year 2100	simultaneous maximal reductions in BC, OC and SO$_2$
SIM5	RCP2.6 year 2100	RCP2.6 year 2100 BC by multiplying the ratios of the emissions of OC and SO$_2$ with BC in 2000	maximal reduction in BC; simultaneous reductions of OC and SO$_2$ in terms of their ratios with BC in recent past
SIM6	RCP4.5 year 2100	RCP4.5 year 2100	medium-low reductions in BC, OC and SO$_2$
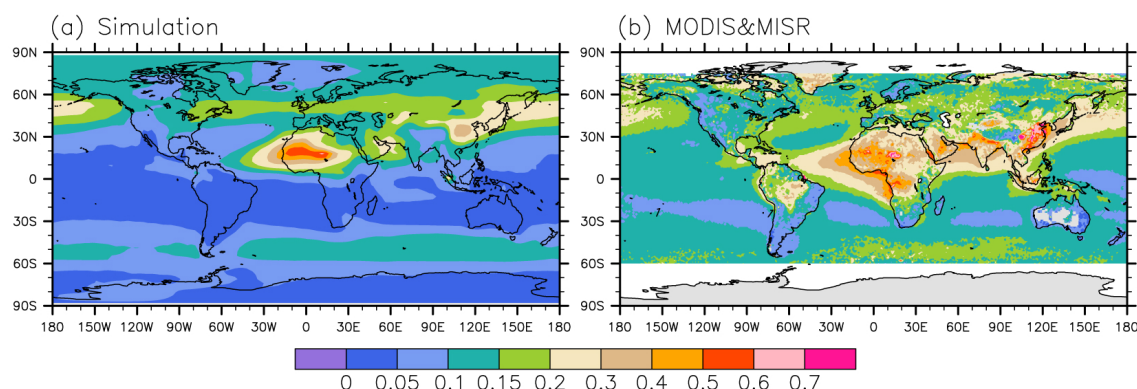
Figure 1. Global distributions of simulated and observed annual mean aerosol optical depth (AOD) at 550 nm. **(a)** Simulation and **(b)** MODIS&MISR (van Donkelaar et al., 2010).

aerosol scattering and absorption excluded; Δ is the difference between 2000 and 2100. The change in cloud radiative forcing (CRF) was used as an approximate way of quantifying the change in combination of the aerosol semi-direct and indirect effects:

$$\Delta CRF = \Delta(F - F_{clear}),\tag{2}$$

where F_{clear} is the flux calculated as a diagnostic with clouds neglected. The change in aerosol net effect was assessed by the change in net radiation flux at the TOA (ΔF) (Ghan et al., 2012). We didn't perform additional simulations in which aerosol scattering and absorption were neglected to exclusively diagnose the effect of aerosols on CRF according to the method by Ghan et al. (2012) and Ghan (2013). Thus, the difference in aerosol net effect is not equal to the sum of ΔADE and ΔCRF in this study.

3 Results

3.1 Aerosol optical depth for present-day conditions

The simulation performance of BCC_AGCM2.0.1_CUACE/Aero has been given by Z. L. Wang et al. (2014) in detail. They demonstrated that the model has a good ability to simulate aerosols, cloud properties, and meteorological fields. However, we replace the aerosol emission from AeroCom with those given by Lamarque et al. (2010) for present-day conditions in this work. Thus, a comparison of simulated annual mean aerosol optical depth (AOD) with satellite retrievals is shown in Fig. 1. The simulated AODs range from 0.3 to 0.6 over the Sahara Desert and are from 0.15 to 0.3 in nearby Arabian areas due to the large dust loading. The AODs are mainly between 0.2 and 0.4 in eastern China, and exceed 0.15 in eastern North America and West Europe due to the large emissions of anthropogenic aerosols. The AODs are above 0.1 over most subtropical oceans because of the contribution of sea salt and sulphate. The model generally reproduces the geographical distribution of AOD well, but it significantly underestimates the

Table 2. Global amounts of aerosol emissions and annual means of aerosol burdens.

	SIM1	SIM2	SIM3	SIM4	SIM5	SIM6
Emission (Tg yr^{-1})						
SO$_2$	107.4	107.4	25.7	12.9	19.8	22.2
BC	7.8	3.3	3.3	3.3	3.3	4.3
OC	35.8	35.8	23.9	25.3	24.9	20.0
Burden (mg m^{-2})						
Sulphate	3.5	3.4	1.3	0.98	1.1	1.2
BC	0.17	0.079	0.078	0.077	0.078	0.084
OC	1.6	1.6	1.2	1.2	1.2	1.1
Dust	39.9	39.9	39.9	40.6	42.7	42.8
Sea salt	14.2	14.2	14.0	14.0	14.0	14.1

Table 3. Global annual mean differences of aerosol direct (DRF), semi-direct and indirect (CRF), and net effect at the TOA (FNT) (positive values mean incoming, units: W m^{-2}) in different simulations*.

	SIM1	ΔSIM2	ΔSIM3	ΔSIM4	ΔSIM5	ΔSIM6
DRF	−2.01	−0.07 ± 0.05	+0.27 ± 0.03	+0.28 ± 0.05	+0.25 ± 0.03	+0.3 ± 0.02
SWCF	−49.0	−0.14 ± 0.2	+0.87 ± 0.3	+1.3 ± 0.14	+1.1 ± 0.17	+1.02 ± 0.2
LWCF	+27.8	+0.03 ± 0.09	−0.07 ± 0.08	−0.2 ± 0.1	−0.19 ± 0.08	−0.14 ± 0.1
CRF	−21.2	−0.11 ± 0.17	+0.8 ± 0.3	+1.1 ± 0.1	+0.91 ± 0.11	+0.88 ± 0.18
FNT	−0.66	−0.12 ± 0.28	+1.7 ± 0.2	+2.0 ± 0.19	+1.8 ± 0.14	+1.8 ± 0.21

* DRF, SWCF, LWCF and CRF, and FNT in the SIM1 column are aerosol direct radiative forcing, shortwave, longwave and net cloud radiative forcing, and net radiation flux at the TOA (units: W m^{-2}) in SIM1, respectively. Values in the ΔSIM2–ΔSIM6 columns represent the changes of corresponding variables in these simulations vs. those in SIM1.

AODs over South Asia, eastern China, and tropical oceans. These errors could be caused by several factors such as uncertainties in the aerosol sources, coarse model resolution, the uncertainties of physical processes, and the absence of nitrate, ammonium and secondary organic aerosols in the model (Zhang et al., 2012a).

3.2 The effect of aerosol reductions

3.2.1 Global mean statistics

Tables 2 and 3 show the global emission amounts and annual mean column burdens of aerosols in all simulations and differences in AREs among them. The global emission amount of BC is reduced from 7.8 Tg yr^{-1} at present to 3.3 Tg yr^{-1} at the end of this century under the RCP2.6 scenario due to the operation of various control measures. The global annual mean of simulated BC burden is decreased from 0.17 mg m^{-2} in SIM1 to 0.08 mg m^{-2} in SIM2, assuming that only BC emission is reduced under the RCP2.6 scenario (Table 2). The reduction in the mass concentration of atmospheric BC results in less direct absorption of solar radiation by atmospheric aerosols, thereby causing the global annual mean aerosol direct radiative effect at the TOA to be enhanced by 0.07 W m^{-2}. This indicates that the net cooling effect is enhanced. The multi-model comparison showed

that our model had much lower normalized radiative forcing for BC than most of the other models (Myhre et al., 2013a). Thus, the change in aerosol direct radiative effect is quite small despite the strong emission reduction for BC. The reduction in the BC concentration also weakens the aerosol semi-direct effect, resulting in an increase of 0.11 W m^{-2} in the absolute value of the global annual mean net CRF (Table 3). Of this increase, the shortwave cloud forcing (SWCF) and longwave cloud forcing (LWCF) components are enhanced by 0.14 and 0.03 W m^{-2}, respectively. It is noted that the change in CRF is a combined effect of decrease in cloud evaporation and increase in cloud cover caused by declining BC, changes in other aerosol concentrations due to adjustment of the atmosphere to BC reduction, and the resulting changes in cloud properties. However, the slight decrease in the sulphate mass concentration due to changes in meteorological fields caused by BC reduction partially offsets the net cooling effect in SIM2 compared with SIM1. Consequently, the global annual mean aerosol net cooling effect at the TOA is enhanced by 0.12 W m^{-2} compared with recent past levels when just BC emission is reduced to the level projected for the end of this century under the RCP2.6 scenario (Table 3).

Many previous studies mentioned in Sect. 1 have indicated that there are several common sources of SO$_2$, BC, and OC (Reddy and Venkataraman, 2002; Zhang et al., 2009; Lamar-
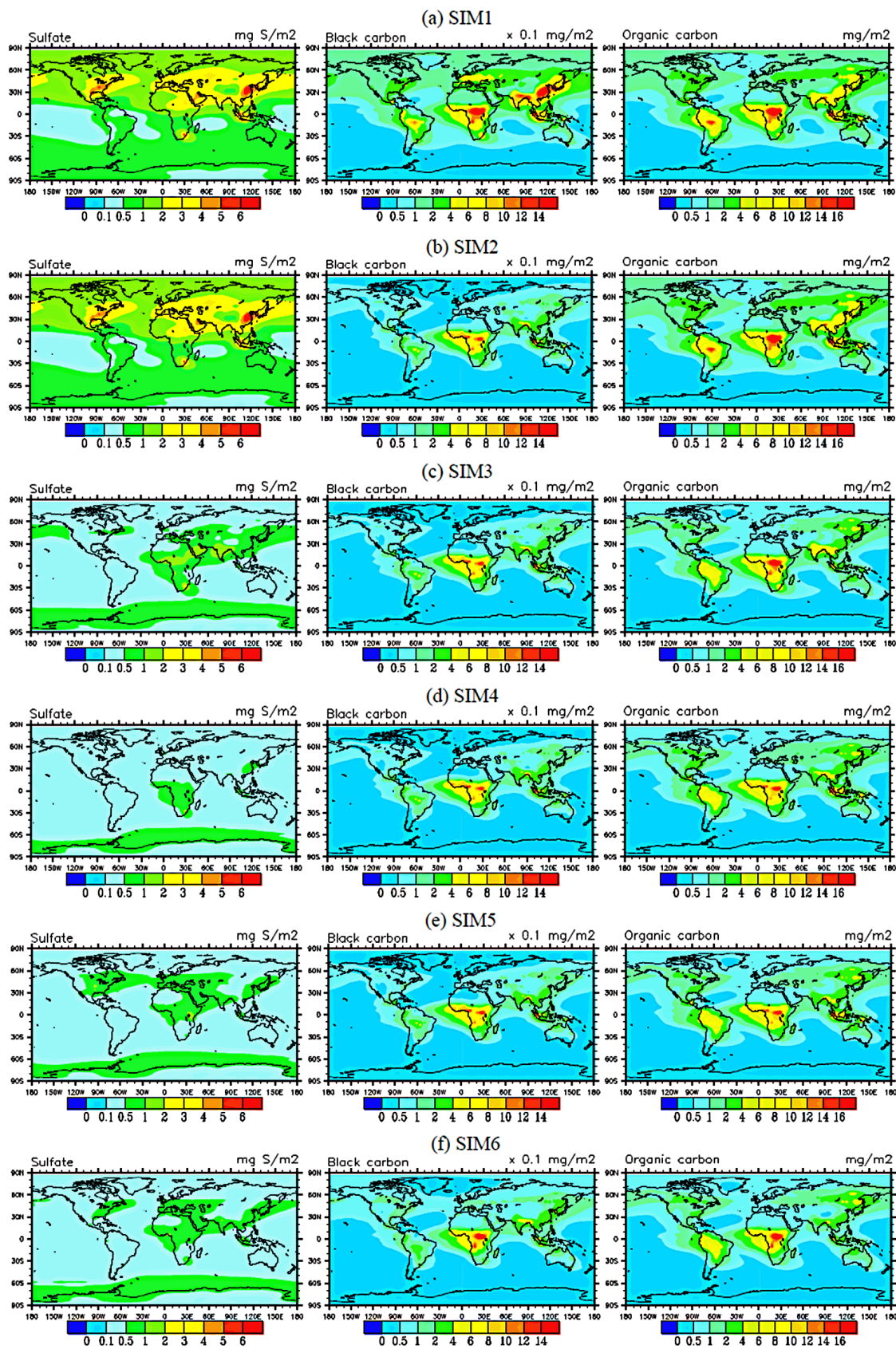
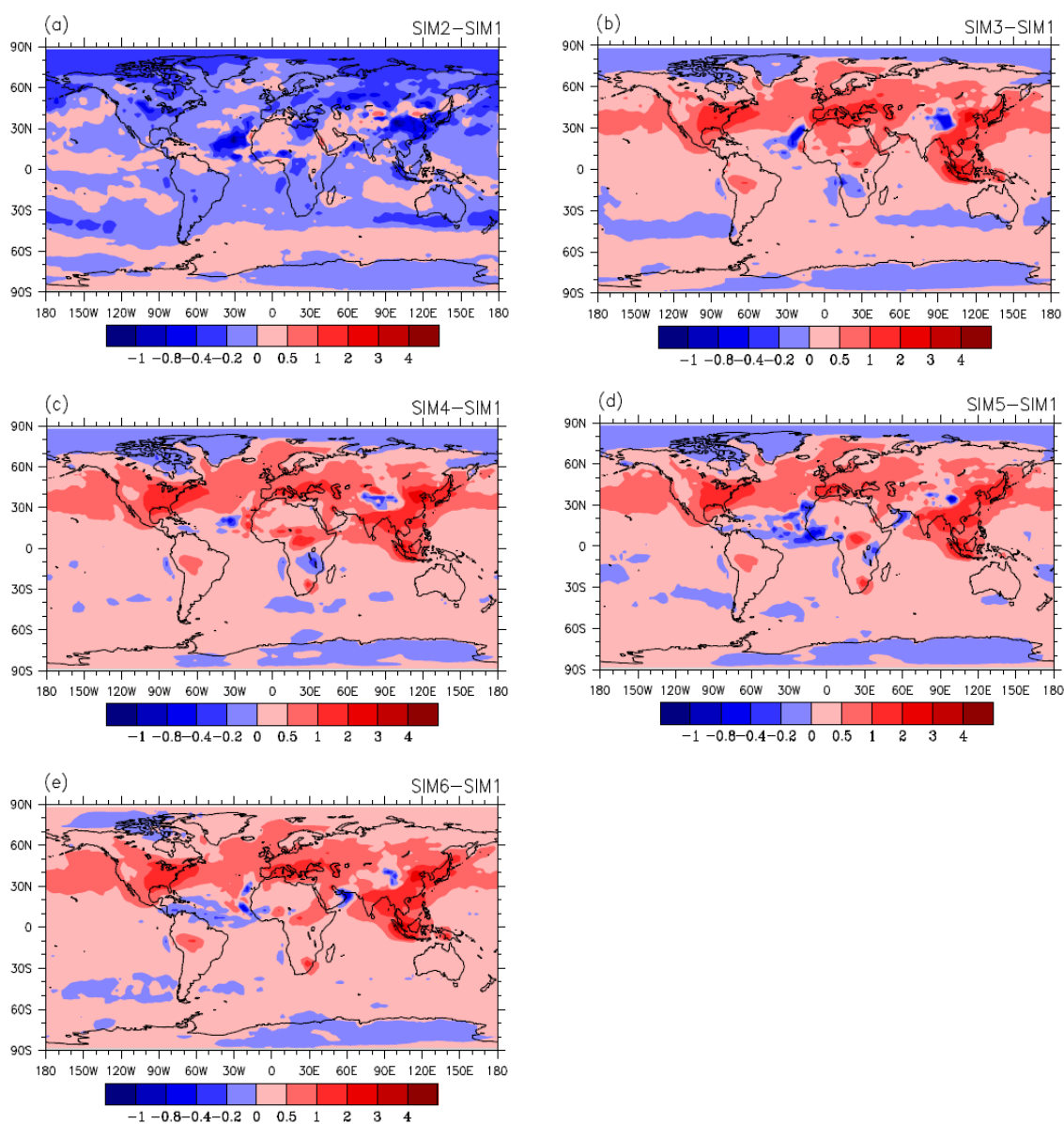**Figure 2.** Global distributions of simulated annual mean aerosol column burdens (units: $\mathrm{mg\,m^{-2}}$).

Figure 3. Global distributions of difference in simulated annual mean aerosol direct effect (units: W m^{-2}). **(a)** SIM2–SIM1, **(b)** SIM3–SIM1, **(c)** SIM4–SIM1, **(d)** SIM5–SIM1, and **(e)** SIM6–SIM1.

que et al., 2010; Chin et al., 2014). SO$_2$ and OC emissions are likely to be reduced proportionally when BC emission is decreased, as there is no effective way of removing BC exclusively without influencing the other co-emitted components. Therefore, we considered four different ways to simultaneously reduce the emissions of SO$_2$, BC, and OC to the levels projected for the end of this century under the RCP2.6, RCP4.5, and RCP8.5 scenarios. Then, we calculated the effects of emission reductions of all these aerosols on radiation fluxes in SIM3 to SIM6. It can be seen from Table 2 that the global emissions of SO$_2$, BC, and OC are decreased to 12.9–25.7, 3.3–4.3, and 20.0–25.3 Tg yr^{-1} under these three scenarios, respectively. Thus, the global annual mean bur-

dens of sulphate, BC, and OC are reduced by different levels (63–72, 51–55, and 25–31 %, respectively). The concurrent reductions in scattering sulphate and OC burdens weaken the global annual mean aerosol direct radiative effect at the TOA by 0.25–0.3 W m^{-2}, although the absorbing BC burden is also significantly reduced in SIM3 to SIM6. Additionally, sulphate and OC particles can act as CCN due to their hygroscopicity, so any decrease in their emissions would decrease CCN concentrations, then decreasing cloud lifetime and albedo, thereby weakening the negative SWCF. As can be seen from Table 3, the absolute values of the global annual mean SWCF are weakened by 0.87–1.3 W m^{-2} due to simultaneous reductions in emissions of SO$_2$, BC, and OC.
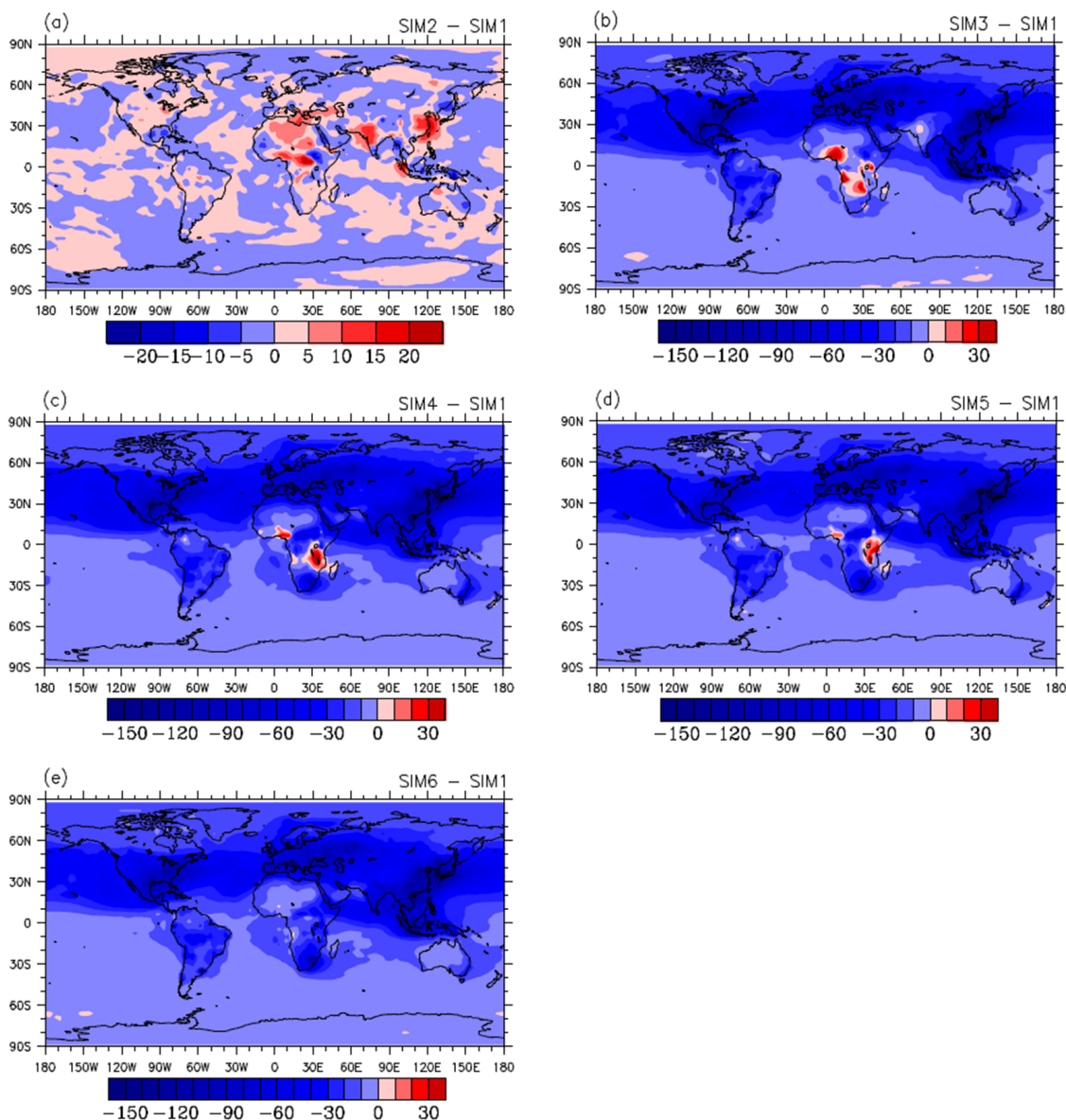
Figure 4. Global distributions of difference in simulated annual mean CCN concentration at surface (units: cm^{-3}). **(a)** SIM2–SIM1, **(b)** SIM3–SIM1, **(c)** SIM4–SIM1, **(d)** SIM5–SIM1, and **(e)** SIM6–SIM1.

The quick adjustment of the atmosphere to aerosol effects leads to changes in LWCF, causing the longwave cooling by 0.07–0.2 W m^{-2} in SIM3 to SIM6 compared with SIM1. It partly offsets the shortwave warming. The absolute values of global annual mean net CRF are decreased by 0.8–1.1 W m^{-2} in SIM3 to SIM6 compared with SIM1, which greatly exceed the changes in the aerosol direct radiative effect. This is consistent with results obtained by Chen et al. (2010), who reported that a reduction in BC emission would dampen aerosol indirect forcing. Finally, the global annual mean aerosol net cooling effect at the TOA is weakened by 1.7–2.0 W m^{-2} when the emissions of SO$_2$, BC, and OC are simultaneously reduced to the levels projected for the

end of this century based on three different RCP scenarios (Table 3).

3.2.2 Global distributions

Figure 2 shows the global distributions of simulated annual mean sulphate, BC, and OC burdens under all six simulations. As can be seen from Fig. 2b, the BC column burdens are significantly decreased in areas with high BC emission such as East Asia, South Asia, central Africa and South America, eastern North America, and Western Europe compared with recent past levels when the emission of only BC is reduced. Changes in other aerosol burdens are
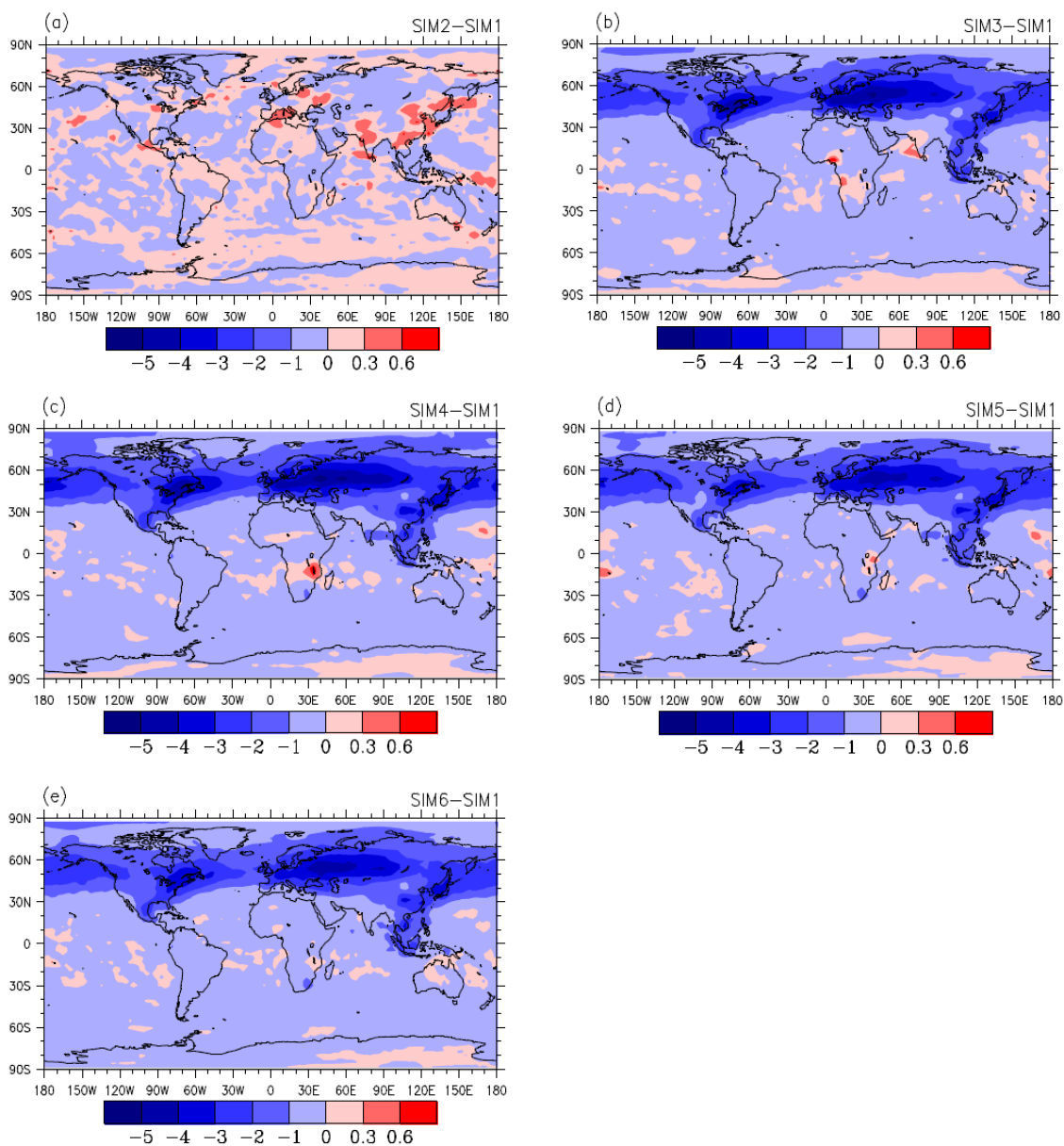
Figure 5. Global distributions of difference in simulated annual mean column CDNC (units: $10^{10}\,\mathrm{m}^{-2}$). **(a)** SIM2–SIM1, **(b)** SIM3–SIM1, **(c)** SIM4–SIM1, **(d)** SIM5–SIM1, and **(e)** SIM6–SIM1.

not obvious. The reduction in the BC concentration weakens the direct absorption of solar radiation by atmospheric aerosols, leading to a cooling effect at the TOA in these regions. The largest cooling exceeds $1\,\mathrm{W\,m}^{-2}$ in China, Europe, and eastern North America (Fig. 3a). The numbers of activated sulphate, OC, and dust particles are increased over East and South Asia, Mediterranean regions, North America and Africa due to the fast adjustment in meteorological fields caused by declining BC (figure not shown), which leads to the increase in CCN concentration (Fig. 4a). Higher CCN concentrations can produce more cloud droplet numbers, with the maximum increase in annual mean column

cloud droplet number concentrations (CDNCs) being up to $0.6 \times 10^{10}\,\mathrm{m}^{-2}$ (Fig. 5a). This enhances the negative SWCF over those regions (Fig. 6a). In addition, the decrease in the absorption ability of aerosols weakens the cloud evaporation and increases the cloud fraction, which further enhances the negative SWCF over the regions with high BC emission and some oceans (Fig. 6a). However, the LWCF is also increased over most areas with enhanced negative SWCF (Fig. 6a), which can partly offset the shortwave cooling. Finally, only the reduction of BC emission results in an increase of more than $2\,\mathrm{W\,m}^{-2}$ in the annual mean aerosol net cooling effect at the TOA over most regions with large BC emission (Fig. 7a).
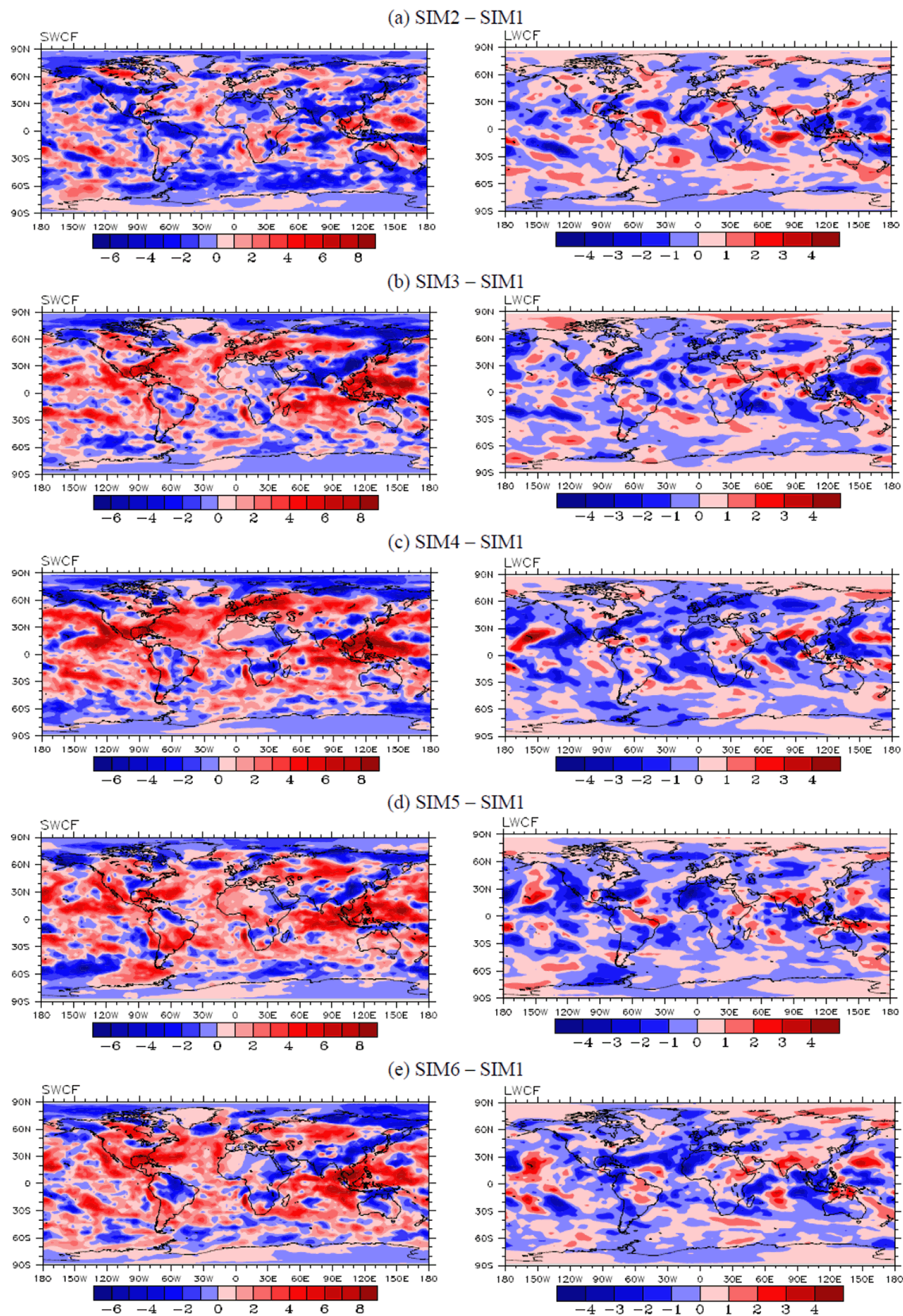
Figure 6. Global distributions of difference in simulated annual mean SWCF and LWCF (units: W m^{-2}). **(a)** SIM2–SIM1, **(b)** SIM3–SIM1, **(c)** SIM4–SIM1, **(d)** SIM5–SIM1, and **(e)** SIM6–SIM1.
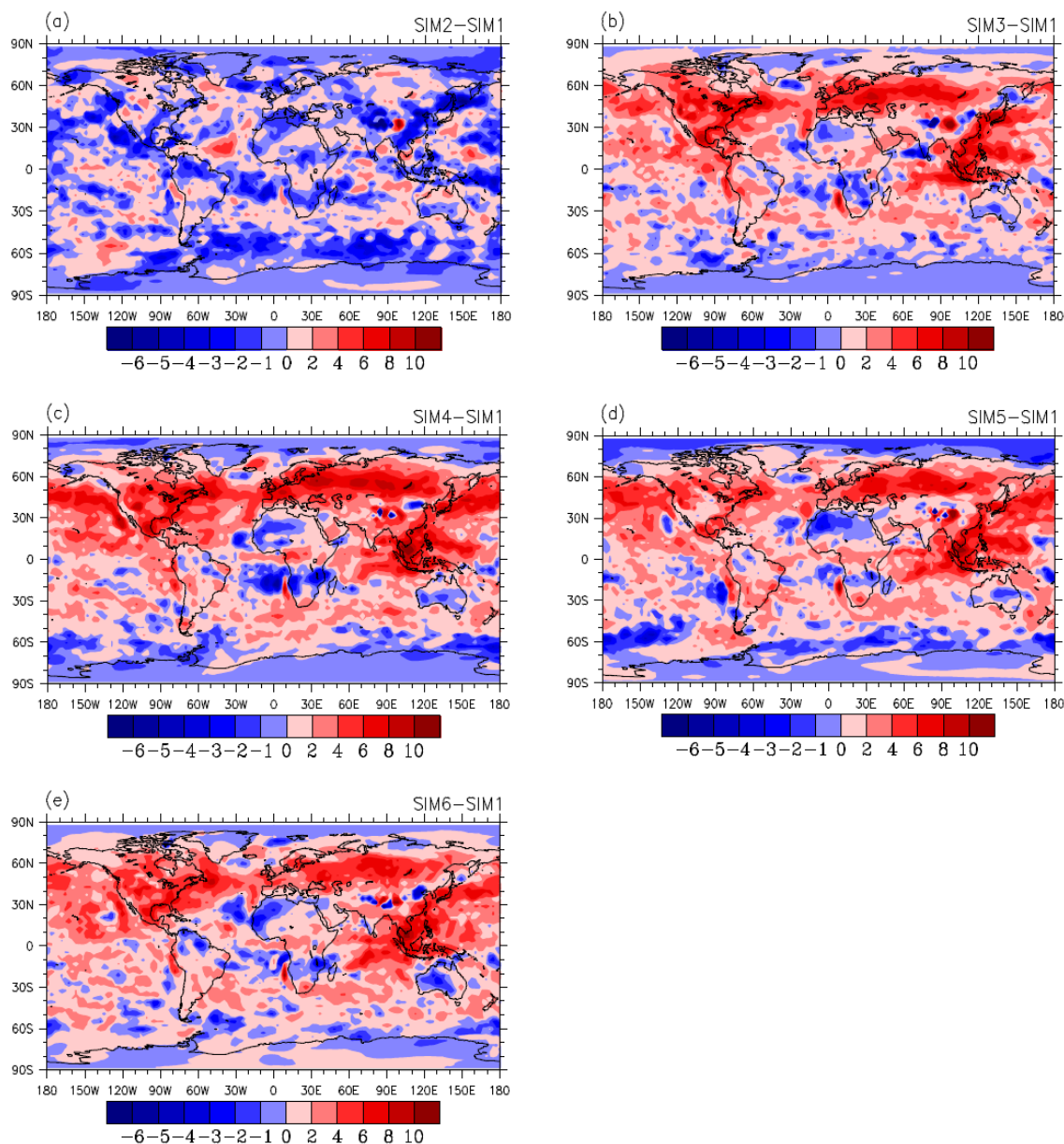
Figure 7. Global distributions of difference in simulated annual mean aerosol net effect (units: $W\,m^{-2}$). **(a)** SIM2–SIM1, **(b)** SIM3–SIM1, **(c)** SIM4–SIM1, **(d)** SIM5–SIM1, and **(e)** SIM6–SIM1.

Figure 2c–f show that there are different levels of reduction in the annual mean sulphate, BC, and OC burdens in SIM3 to SIM6, with decreases of up to 2.0–$5.0\,mg\,S\,m^{-2}$, 0.2–1.0 and 2.0–$6.0\,mg\,m^{-2}$ in most areas, respectively, when all aerosol emissions are reduced. The combined reduction in scattering and absorbing aerosols weakens the aerosol direct radiative effect at the TOA by over $1\,W\,m^{-2}$ for most of the Northern Hemisphere (NH) compared with SIM1 (Fig. 3b–e). The CCN concentrations are greatly decreased over the globe, except for individual regions, mainly due to the emission reductions in hygroscopic sulphate and OC, especially over the middle latitudes of the NH (Fig. 4b–

e). Correspondingly, the CDNCs are significantly decreased in SIM3 to SIM6 compared with SIM1. The largest decreases in annual mean column CDNCs exceed $5 \times 10^{10}\,m^{-2}$ in Western Europe, North America, and eastern China (Fig. 5b–e). Decreased CDNCs can decrease the cloud albedo and lifetime and weaken the negative SWCF in the regions with high anthropogenic aerosol emissions such as North America and Europe (Fig. 6b–e). The negative SWCFs are enhanced due to the increase in low cloud fraction over most of South and East Asia, though the CCNs are clearly decreased. The shortwave warmings (coolings) are also compensated by the longwave coolings (warmings) over most regions (Fig. 6b–

e). Finally, the annual mean aerosol net cooling effect at the TOA is weakened over a range of 2.0–10.0 W m^{-2} due to the changes in emissions of all aerosols over most regions of the NH that have large anthropogenic aerosol emissions (Fig. 7b–e).

4 Discussion and conclusions

It has been argued that eliminating BC emission would be an effective measure to slow down global warming and environmental pollution. In this study, we assess the impact of removing some sources of BC and other co-emitted species on aerosol radiative effects by using an aerosol–climate atmosphere-only model BCC_AGCM2.0.1_CUACE/Aero with prescribed SST and SIC, in combination with the RCP scenarios. Compared with the aerosol effect for recent past, the global annual mean aerosol net cooling effect at the TOA is enhanced by 0.12 W m^{-2} due to a decrease in the direct absorption of solar radiation and aerosol semi-direct effect when BC emission is reduced exclusively to the level projected for the end of this century under the RCP2.6 scenario. The annual mean aerosol net cooling effect at the TOA is enhanced by more than 2.0 W m^{-2} in eastern China, northern India, and Mediterranean regions. Therefore, a reduction of BC emission alone could ideally mitigate global warming.

However, our results suggest that associating with the reduction of net cooling effects directly from aerosols, the aerosol indirect effect is also weakened when emissions of SO$_2$, BC, and OC are simultaneously reduced in different ways to the levels projected for the end of this century under the RCP2.6, RCP4.5, and RCP8.5 scenarios. Relative to the aerosol effect for recent past, the total global annual mean aerosol net cooling effect at the TOA is weakened by 1.7–2.0 W m^{-2} with the reduction according to potential actual conditions in the emission of all these aerosols (i.e., BC and the major co-emitted species). The main cooling regions are over East Asia, Western Europe, eastern North America, and central Africa, with the largest change exceeding 10.0 W m^{-2}. This is somewhat consistent with the results given by Gillett and Salzen (2013) and Levy et al. (2013), who also reported that the reduction in atmospheric aerosols will weaken the aerosol cooling effect in the future.

This study highlights that reducing only BC emission could play a positive role in mitigating global warming and environmental pollution, and would be beneficial to human health. However, the emissions of some co-emitted scattering aerosols and their precursor gases will be inevitably reduced when BC emission is reduced due to their homology. Therefore, reducing BC emission could lead to unexpected warming on the Earth's climate in the future, unless certain technical advances in emission reduction technology are available for removal of the BC exclusively without influencing the other co-emitted components.

There exists large uncertainty in BC radiative forcing (Bond et al., 2013; Boucher et al., 2013; Myhre et al., 2013a, b). One reason for the uncertainty is from the biases of current emission inventories of BC, mostly obtained from the so-called bottom-up approach (Cohen and Wang, 2014). Cohen and Wang (2014) provided a global-scale top-down estimation of BC emissions, a factor of more than 2 higher than commonly used global BC emissions data sets, by using a Kalman Filter method. If present-day BC emissions have been substantially underestimated, increase in aerosol net cooling effect may be larger due to only reduction in BC emission. Furthermore, co-emissions of other compounds with BC, such as CO$_2$, might be more important than SO$_2$ and OC (Rogelj et al., 2014). The reduction in CO$_2$ can mitigate global warming when reducing BC. However, it is very difficult to fully obtain the ratios of BC with its co-emitted components due to the complexity of emission sources and diversity of energy structure in different regions. These bring about large uncertainties for the relevant research.

Because of the potential uncertainties mentioned above, we need to continuously improve our understanding on emissions of BC and its co-emitted species through a lot of observation and analysis. We also encourage other modeling groups to perform similar simulations to check the robustness of these results.

References

Abdul-Razzak, H. and Ghan, S. J.: A parameterization of aerosol activation, 2. Multiple aerosol types, J. Geophys. Res., 105, 6837–6844, doi:10.1029/1999JD901161, 2000.

Albrecht, B.: Aerosols, cloud microphysics, and fractional cloudiness, Science, 245, 1227–1230, doi:10.1126/science.245.4923.1227, 1989.

Bond, T. C., Streets, D. G., Yarber, K. F., Nelson, S. M., Woo, J.-H., and Klimont, Z.: A technology-based global inventory of black and organic carbon emissions from combustion, J. Geophys. Res., 109, D14203, doi:10.1029/2003JD003697, 2004.

Bond, T. C., Doherty, S. J., Fahey, D. W., Forster, P. M., Berntsen, T., DeAngelo, B. J., Flanner, M. G., Ghan, S., Kärcher, B., Koch, D., Kinne, S., Kondo, Y., Quinn, P. K., Sarofim, M. C., Schultz, M. G., Schulz, M., Venkataraman, C., Zhang, H., Zhang, S., Bellouin, N., Guttikunda, S. K., Hopke, P. K., Jacobson, M. Z., Kaiser, J. W., Klimont, Z., Lohmann, U., Schwarz, J. P., Shindell, D., Storelvmo, T., Warren, S. G., and Zender, C. S.: Bounding the role of black carbon in the climate system:

a scientific assessment, J. Geophys. Res.-Atmos., 118, 1–173, doi:10.1002/jgrd.50171, 2013.

Boucher, O., Randall, D., Artaxo, P., Bretherton, C., Feingold, G., Forster, P., Kerminen, V.-M., Kondo, Y., Liao, H., Lohmann, U., Rasch, P., Satheesh, S. K., Sherwood, S., Stevens, B., and Zhang, X. Y.: Clouds and aerosols, in: Climate Change 2013: The Physical Science Basis. Contribution of Working Group I to the Fifth Assessment Report of the Intergovernmental Panel on Climate Change, edited by: Stocker, T. F., Qin, D., Plattner, G.-K., Tignor, M., Allen, S. K., Boschung, J., Nauels, A., Xia, Y., Bex, V., and Midgley, P. M., Cambridge Univ. Press, Cambridge, UK, New York, NY, USA, 573–632, 2013.

Chen, W.-T., Lee, Y. H., Adams, P. J., Nenes, A., and Seinfeld, J. H.: Will black carbon mitigation dampen aerosol indirect forcing?, Geophys. Res. Lett., 37, L09801, doi:10.1029/2010GL042886, 2010.

Chin, M., Diehl, T., Tan, Q., Prospero, J. M., Kahn, R. A., Remer, L. A., Yu, H., Sayer, A. M., Bian, H., Geogdzhayev, I. V., Holben, B. N., Howell, S. G., Huebert, B. J., Hsu, N. C., Kim, D., Kucsera, T. L., Levy, R. C., Mishchenko, M. I., Pan, X., Quinn, P. K., Schuster, G. L., Streets, D. G., Strode, S. A., Torres, O., and Zhao, X.-P.: Multi-decadal aerosol variations from 1980 to 2009: a perspective from observations and a global model, Atmos. Chem. Phys., 14, 3657–3690, doi:10.5194/acp-14-3657-2014, 2014.

Chuang, C. C., Penner, J. E., Prospero, J. M., Grant, K. E., Rau, G. H., and Kawamoto, K.: Cloud susceptibility and the first aerosol indirect forcing: sensitivity to black carbon and aerosol concentrations, J. Geophys. Res., 107, 4564, doi:10.1029/2000JD000215, 2002.

Cohen, J. B. and Wang, C.: Estimating global black carbon emissions using a top-down Kalman Filter approach, J. Geophys. Res.-Atmos., 119, 307–323, doi:10.1002/2013JD019912, 2014.

d'Almeida, G. A., Koepke, P., and Shettle, E.: Atmospheric Aerosols: Global Climatology and Radiative Forcing, 561 pp., A. Deepak, Hampton, Va, 1991.

DeMott, P. J., Rogers, D. C., and Kreidenweis, S. M.: The susceptibility of ice formation in upper tropospheric clouds to insoluble aerosol components, J. Geophys. Res., 102, 19575–19584, doi:10.1029/97JD01138, 1997.

Ghan, S. J.: Technical Note: Estimating aerosol effects on cloud radiative forcing, Atmos. Chem. Phys., 13, 9971–9974, doi:10.5194/acp-13-9971-2013, 2013.

Ghan, S. J., Liu, X., Easter, R. C., Zaveri, R., Rasch, P. J., Yoon, J.-H., and Eaton, B.: Toward a minimal representation of aerosols in climate models: Comparative decomposition of aerosol direct, semi-direct and indirect radiative forcing, J. Climate, 25, 6461–6476, doi:10.1175/JCLI-D-11-00650.1, 2012.

Gillett, N. P. and Salzen, K. V.: The role of reduced aerosol precursor emissions in driving near-term warming, Environ. Res. Lett., 8, 034008, doi:10.1088/1748-9326/8/3/034008, 2013.

Gong, S. L., Barrie, L. A., and Lazare, M.: Canadian Aerosol Module (CAM): a size-segregated simulation of atmospheric aerosol processes for climate and air quality models, 2. Global seasalt aerosol and its budgets, J. Geophys. Res., 107, 4779, doi:10.1029/2001JD002004, 2002.

Gong, S. L., Barrie, L. A., Blanchet, J.-P., Salzen, K. V., Lohmann, U., Lesins, G., Spacek, L., Zhang, L. M., Girard, E., Lin, H., Leaitch, R., Leighton, H., Chylek, P., and Huang, P.: Canadian Aerosol Module: a size-segregated simulation of atmo-

spheric aerosol processes for climate and air quality models 1. Module development, J. Geophys. Res., 108, 4007, doi:10.1029/2001JD002002, 2003.

Hansen, J., Sato, M., Ruedy, R., Lacis, A., and Oinas, V.: Global warming in the twenty-first century: an alternative scenario, P. Natl. Acad. Sci. USA, 97, 9875–9880, 2000.

Hodnebrog, Ø., Myhre, G., and Samset, B. H.: How shorter black carbon lifetime alters its climate effect, Nature Communications, 5, 5065, doi:10.1038/ncomms6065, 2014.

Hurrell, J. W., Hack, J. J., Shea, D., Caron, J. M., and Rosinski, J.: A new sea surface temperature and sea ice boundary dataset for the Community Atmosphere Model, J. Climate, 21, 5145–5153, 2008.

Jacobson, M. Z.: Short-term effects of controlling fossil-fuel soot, biofuel soot and gases, and methane on climate, Arctic ice, and air pollution health, J. Geophys. Res., 115, D14209, doi:10.1029/2009JD013795, 2010.

Jacobson, M. Z.: Investigating cloud absorption effects: Global absorption properties of black carbon, tar balls, and soil dust in clouds and aerosols, J. Geophys. Res., 117, D06205, doi:10.1029/2011JD017218, 2012.

Jing, X. and Zhang, H.: Application and evaluation of McICA scheme in BCC_AGCM2.0.1, AIP Conf. Proc., 1531, 756, doi:10.1063/1.4804880, 2013.

Koch, D. and Del Genio, A. D.: Black carbon semi-direct effects on cloud cover: review and synthesis, Atmos. Chem. Phys., 10, 7685–7696, doi:10.5194/acp-10-7685-2010, 2010.

Lamarque, J.-F., Bond, T. C., Eyring, V., Granier, C., Heil, A., Klimont, Z., Lee, D., Liousse, C., Mieville, A., Owen, B., Schultz, M. G., Shindell, D., Smith, S. J., Stehfest, E., Van Aardenne, J., Cooper, O. R., Kainuma, M., Mahowald, N., McConnell, J. R., Naik, V., Riahi, K., and van Vuuren, D. P.: Historical (1850–2000) gridded anthropogenic and biomass burning emissions of reactive gases and aerosols: methodology and application, Atmos. Chem. Phys., 10, 7017–7039, doi:10.5194/acp-10-7017-2010, 2010.

Lee, Y. H., Lamarque, J.-F., Flanner, M. G., Jiao, C., Shindell, D. T., Berntsen, T., Bisiaux, M. M., Cao, J., Collins, W. J., Curran, M., Edwards, R., Faluvegi, G., Ghan, S., Horowitz, L. W., McConnell, J. R., Ming, J., Myhre, G., Nagashima, T., Naik, V., Rumbold, S. T., Skeie, R. B., Sudo, K., Takemura, T., Thevenon, F., Xu, B., and Yoon, J.-H.: Evaluation of preindustrial to present-day black carbon and its albedo forcing from Atmospheric Chemistry and Climate Model Intercomparison Project (ACCMIP), Atmos. Chem. Phys., 13, 2607–2634, doi:10.5194/acp-13-2607-2013, 2013.

Levy, H., Horowitz, L. W., Schwarzkopf, M. D., Ming, Y., Golaz, J.-C., Naik, V., and Ramaswamy, V.: The roles of aerosol direct and indirect effects in past and future climate change, J. Geophys. Res.-Atmos., 118, 4521–4532, doi:10.1002/jgrd.50192, 2013.

Morrison, H. and Gettelman, A.: A new two-moment bulk stratiform cloud microphysics scheme in the Community Atmosphere Model, version 3 (CAM3), part I: description and numerical tests, J. Climate, 21, 3642–3659, 2008.

Myhre, G., Samset, B. H., Schulz, M., Balkanski, Y., Bauer, S., Berntsen, T. K., Bian, H., Bellouin, N., Chin, M., Diehl, T., Easter, R. C., Feichter, J., Ghan, S. J., Hauglustaine, D., Iversen, T., Kinne, S., Kirkevåg, A., Lamarque, J.-F., Lin, G., Liu, X., Lund, M. T., Luo, G., Ma, X., van Noije, T., Penner, J. E., Rasch,

P. J., Ruiz, A., Seland, Ø., Skeie, R. B., Stier, P., Takemura, T., Tsigaridis, K., Wang, P., Wang, Z., Xu, L., Yu, H., Yu, F., Yoon, J.-H., Zhang, K., Zhang, H., and Zhou, C.: Radiative forcing of the direct aerosol effect from AeroCom Phase II simulations, Atmos. Chem. Phys., 13, 1853–1877, doi:10.5194/acp-13-1853-2013, 2013a.

Myhre, G., Shindell, D., Bréon, F.-M., Collins, W., Fuglestvedt, J., Huang, J., Koch, D., Lamarque, J.-F., Lee, D., Mendoza, B., Nakajima, T., Robock, A., Stephens, G., Takemura, T., and Zhang, H.: Anthropogenic and natural radiative forcing, in: Climate Change 2013: The Physical Science Basis. Contribution of Working Group I to the Fifth Assessment Report of the Intergovernmental Panel on Climate Change, edited by: Stocker, T. F., Qin, D., Plattner, G.-K., Tignor, M., Allen, S. K., Boschung, J., Nauels, A., Xia, Y., Bex, V., and Midgley, P. M., Cambridge Univ. Press, Cambridge, UK, New York, NY, USA, 659–740, 2013b.

Pincus, R., Barker, H. W., and Morcrette, J.-J.: A fast, flexible, approximate technique for computing radiative transfer in inhomogeneous cloud fields, J. Geophys. Res., 108, 4376, doi:10.1029/2002JD003322, 2003.

Ramanathan, V. and Carmichael, G.: Global and regional climate changes due to black carbon, Nature, 1, 221–227, 2008.

Reddy, S. M. and Venkataraman, C.: Inventory of aerosol and sulphur dioxide emissions from India: Part I – fossil fuel combustion, Atmos. Environ., 36, 677–697, 2002.

Rogelj, J., Schaeffer, M., Meinshausen, M., Shindell, D. T., Hare, W., Klimont, Z., Velders, G. J. M., Amann, M., and Schellnhuber, H. J.: Disentangling the effects of CO_2 and short-lived climate forcer mitigation, P. Natl. Acad. Sci. USA, 111, 46, 16325–16330, doi:10.1073/pnas.1415631111, 2014.

Samset, B. H., Myhre, G., Herber, A., Kondo, Y., Li, S.-M., Moteki, N., Koike, M., Oshima, N., Schwarz, J. P., Balkanski, Y., Bauer, S. E., Bellouin, N., Berntsen, T. K., Bian, H., Chin, M., Diehl, T., Easter, R. C., Ghan, S. J., Iversen, T., Kirkevåg, A., Lamarque, J.-F., Lin, G., Liu, X., Penner, J. E., Schulz, M., Seland, Ø, Skeie, R. B., Stier, P., Takemura, T., Tsigaridis, K., and Zhang, K.: Modeled black carbon radiative forcing and atmospheric lifetime in AeroCom Phase II constrained by aircraft observations, Atmos. Chem. Phys. Discuss., 14, 20083–20115, doi:10.5194/acpd-14-20083-2014, 2014.

Shindell, D., Kuylenstierna, J. C. I., Vignati, E., van Dingenen, R., Amann, M., Klimont, Z., Anenberg, S. C., Muller, N., Janssens-Maenhout, G., Raes, F., Schwartz, J., Faluvegi, G., Pozzoli, L, Kupiainen, K., Hoglund-Isaksson, L., Emberson, L., Streets, D., Ramanathan, V., Hicks, K., Kim Oanh, N. T., Milly, G., Williams, M., Demkine, V., and Fowler, D.: Simultaneously mitigating near-term climate change and improving human health and food security, Science, 335, 183–189, doi:10.1126/science.1210026, 2012.

Twomey, S. A.: The influence of pollution on the shortwave albedo of clouds, J. Atmos. Sci., 34, 1149–1152, 1977.

van Donkelaar, A., Martin, R. V., Brauer, M., Kahn, R., Levy, R., Verduzco, C., and Villeneuve, P. J.: Global estimates of ambient fine particulate matter concentrations from satellite-based aerosol optical depth: Development and application, Environ. Health Persp., 118, 847–855, doi:10.1289/ehp.0901623, 2010.

van Vuuren, D. P., Edmonds, J., Kainuma, M., Riahi, K., Thomson, A., Hibbard, K., Hurtt, G. C., Kram, T., Krey, V., and Lamarque, J.-F.: The representative concentration pathways: an overview, Climatic Change, 109, 5–31, doi:10.1007/s10584-011-0148-z, 2011.

Wang, Q., Jacob, D. J., Spackman, J. R., Perring, A. E., Schwarz, J. P., Moteki, N., Marais, E. A., Ge, C., Wang, J., and Barrett, S. R. H.: Global budget and radiative forcing of black carbon aerosol: Constraints from pole-to-pole (HIPPO) observations across the Pacific, J. Geophys. Res.-Atmos., 119, 195–206, doi:10.1002/2013jd020824, 2014.

Wang, Z. L., Zhang, H., and Shen, X. S.: Radiative forcing and climate response due to black carbon in snow and ice, Adv. Atmos. Sci., 28, 1336–1344, doi:10.1007/s00376-011-0117-5, 2011.

Wang, Z. L., Zhang, H., Li, J., Jing, X. W., and Lu, P.: Radiative forcing and climate response due to the presence of black carbon in cloud droplets, J. Geophys. Res., 118, 3662–3675, doi:10.1002/jgrd.50312, 2013a.

Wang, Z. L., Zhang, H., Jing, X. W., and Wei, X. D.: Effect of nonspherical dust aerosol on its direct radiative forcing, Atmos. Res., 120, 112–126, doi:10.1016/j.atmosres.2012.08.006, 2013b.

Wang, Z. L., Zhang, H., and Lu, P.: Improvement of cloud microphysics in the aerosol-climate model BCC_AGCM2.0.1_CUACE/Aero, evaluation against observations, and updated aerosol indirect effect, J. Geophys. Res., 119, 8400–8417, doi:10.1002/2014JD021886, 2014.

Wei, X. D. and Zhang, H.: Analysis of optical properties of nonspherical dust-like aerosols, Acta Optica Sinica, 31, 0501002-1–0501002-8, doi:10.3788/AOS201131.0501002, 2011.

Wu, T., Yu, R. C., Zhang, F., Wang, Z. Z., Dong, M., Wang, L., Jin, X., Chen, D., and Li, L.: The Beijing Climate Center atmospheric general circulation model: description and its performance for the present-day, Clim. Dynam., 34, 123–147, doi:10.1007/s00382-009-0594-8, 2010.

Zhang, H., Nakajima, T., Shi, G. Y., Suzuki, T., and Imasu, R.: An optimal approach to overlapping bands with correlated-k distribution method and its application to radiative transfer calculations, J. Geophys. Res., 108, 4641, doi:10.1029/2002JD003358, 2003.

Zhang, H., Shi, G. Y., Nakajima, T., and Suzuki, T.: The effects of the choice of the k-interval number on radiative calculations, J. Quant. Spectrosc. Ra., 98, 31–43, 2006a.

Zhang, H., Suzuki, T., Nakajima, T., Shi, G. Y., Zhang, X. Y., and Liu, Y.: Effects of band division on radiative calculations, Opt. Eng., 45, 016002, doi:10.1117/1.2160521, 2006b.

Zhang, H., Wang, Z. L., Wang, Z. Z., Liu, Q., Gong, S., Zhang, X. Y., Shen, Z., Lu, P., Wei, X., Che, H., and Li, L.: Simulation of direct radiative forcing of typical aerosols and their effects on global climate using an online AGCM-aerosol coupled model system, Clim. Dynam., 38, 1675–1693, 2012a.

Zhang, H., Shen, Z. P., Wei, X. D., Zhang, M.-G., and Li, Z.: Comparison of optical properties of nitrate and sulfate aerosol and the direct radiative forcing due to nitrate in China, Atmos. Res., 113, 113–125, 2012b.

Zhang, H., Jing, X., and Li, J.: Application and evaluation of a new radiation code under McICA scheme in BCC_AGCM2.0.1, Geosci. Model Dev., 7, 737–754, doi:10.5194/gmd-7-737-2014, 2014.

Zhang, Q., Streets, D. G., Carmichael, G. R., He, K. B., Huo, H., Kannari, A., Klimont, Z., Park, I. S., Reddy, S., Fu, J. S., Chen, D., Duan, L., Lei, Y., Wang, L. T., and Yao, Z. L.: Asian emis-

sions in 2006 for the NASA INTEX-B mission, Atmos. Chem. Phys., 9, 5131–5153, doi:10.5194/acp-9-5131-2009, 2009.

Zhang, X. Y., Wang, Y. Q., Niu, T., Zhang, X. C., Gong, S. L., Zhang, Y. M., and Sun, J. Y.: Atmospheric aerosol compositions in China: spatial/temporal variability, chemical signature, regional haze distribution and comparisons with global aerosols, Atmos. Chem. Phys., 12, 779–799, doi:10.5194/acp-12-779-2012, 2012.

Zhao, S. Y., Zhang, H., Feng, S., and Fu, Q.: Simulating direct effects of dust aerosol on arid and semi-arid regions using an aerosol-climate coupled system, Int. J. Climatol., doi:10.1002/joc.4093, online first, 2014.

Zhou, C. H., Gong, S., Zhang, X.-Y., Liu, H. L., Xue, M., Cao, G. L., An, X. Q., Che, H. Z., Zhang, Y. M., and Niu, T.: Towards the improvements of simulating the chemical and optical properties of Chinese aerosols using an online coupled model-CUACE/Aero, Tellus B, 64, 18965, doi:10.3402/tellusb.v64i0.18965, 2012.